Preparation and characterization of high-density spherical $Li_{0.97}Cr_{0.01}FePO_4$/C cathode material for lithium ion batteries

Jierong Ying [*], Min Lei, Changyin Jiang, Chunrong Wan, Xiangming He,
Jianjun Li, Li Wang, Jianguo Ren

Institute of Nuclear and New Energy Technology, Tsinghua University, P.O. Box 1021, Beijing 102201, PR China

Abstract

$LiFePO_4$ is the new generation cathode material for lithium ion batteries. To improve the powders' pile density is considered as the important researching direction. One effective way is to prepare powders composed of spherical particles. Spherical amorphous $FePO_4 \cdot xH_2O$ powders were synthesized by controlled crystallization method, using $Fe(NO_3)_3$, H_3PO_4 and NH_3 as the raw materials. The $FePO_4 \cdot xH_2O$ powders were pre-heat treated at 520 °C for 20 h in air to obtain spherical hexagonal $FePO_4$ powders. The $FePO_4$ powders were homogeneously mixed with Li_2CO_3, $Cr(NO_3)_3$ and sucrose with certain molar ratios, and then sintered at 800 °C for 16 h in N_2. The spherical olivine $Li_{0.97}Cr_{0.01}FePO_4$/C powders were finally obtained through carbothermal reduction process. The composition, structure, morphology, and physicochemical properties of $FePO_4 \cdot xH_2O$, $FePO_4$ and $Li_{0.97}Cr_{0.01}FePO_4$/C powders were characterized in detail by DTA/TGA, ICP, XRD, SEM, XPS, laser particle size analysis, and tap-density testing. It is observed the tap-density of the spherical $Li_{0.97}Cr_{0.01}FePO_4$/C powders is as high as $1.8 \, g \, cm^{-3}$, which is remarkably higher than the non-spherical $LiFePO_4$ powders reported. At current of 0.005, 0.05, 0.1, 0.25 and 1.0 C, the composite cathode materials have initial discharge specific capacity of 163, 151, 142, 131 and $110 \, mAh \, g^{-1}$, respectively. The material also shows excellent cycling performance. The high-density spherical $Li_{0.97}Cr_{0.01}FePO_4$/C cathode material can be used in the lithium ion batteries to greatly increase the batteries' energy density. To further improve the material's pile density and rate capability is considered as the researching direction.
© 2005 Elsevier B.V. All rights reserved.

Keywords: Lithium ion batteries; Controlled crystallization method; $Li_{0.97}Cr_{0.01}FePO_4$/C; High-density; Spherical

1. Introduction

Recently, olivine-structured $LiFePO_4$ proposed by Padhi et al. [1] is gaining particular interest as a candidate cathode material for lithium ion batteries. Comparing to the commercially used $LiCoO_2$, $LiNiO_2$, $LiMn_2O_4$ and their derivatives, $LiFePO_4$ cathode materials have the outstanding advantages of low cost, excellent heat stability, satisfactory safety and low toxicity, etc.

However, there are two main obstacles preventing $LiFePO_4$ to be put into commercially used. One is the poor electronic conductivity, which leads to initial capacity loss and poor rate capability. The other is the low pile density, which leads to low volumetric specific capacity.

To improve the electronic conductivity, several effective ways have been proposed, including synthesis of $LiFePO_4$/electronic conductor composites [2–5] (carbon or metal nanoparticles), substitution of a small quantity of Li^+ by supervalent metal ions [6,7] (Mg^{2+}, Al^{3+}, Cr^{3+}, Zr^{4+}, Ti^{4+}, Nb^{5+}, W^{6+}), preparation of powders with fine particles [8], etc.

Unfortunately, little attention has been fixed on improving the pile density of $LiFePO_4$ so far. The $LiFePO_4$ powders are usually prepared via conventional solid state reaction of mechanically mixed lithium compounds (typically Li_2CO_3 or $LiOH \cdot H_2O$), iron compounds (typically $FeC_2O_4 \cdot 2H_2O$ or $Fe(OOCCH_3)_2$), and phosphates (typically $NH_4H_2PO_4$ or $(NH_4)_2HPO_4$). The obtained $LiFePO_4$ powders always show irregular particle morphology with broad particle size distribution. According to our test, the tap-density of the powders is usually 1.0–$1.4 \, g \, cm^{-3}$, which is much lower than the tap-density of commercially used $LiCoO_2$ (typically 2.4–$2.6 \, g \, cm^{-3}$). The low density of $LiFePO_4$ cathode materials leads to the low volumetric specific capacity,

* Corresponding author. Tel.: +86 10 82780860/89796085;
fax: +86 10 69771464/89796031.
*E-mail address:* yingjr@mail.tsinghua.edu.cn (J. Ying).

thus seriously limiting the energy density of lithium ion batteries. Since great progress has been made to improve the electronic conductivity of LiFePO$_4$, how to improve the powders' pile density, usually the tap-density, becomes more important and urgent.

As has been reported in our previous publications [9,10], the tap-density of the powders is almost decided by the powders' particle morphology, besides the materials' theoretical density. The powders composed of spherical particles have higher density than the powders composed of irregular particles. Thus, to obtain high density LiFePO$_4$ cathode material, preparing spherical powders is expected as an effective way.

In our laboratory, the high-density spherical LiCoO$_2$ and LiNi$_{0.8}$Co$_{0.2}$O$_2$ cathode materials have been prepared via a controlled crystallization—solid-state reaction method [9,10]. We have also reported a novel controlled crystallization—carbothermal reduction method to synthesize spherical carbon-coated LiFePO$_4$ cathode material in which the carbon content is about 6 wt.% [11]. The spherical carbon-coated LiFePO$_4$ has the high tap-density of 1.6 g cm^{-3}. However, the material has the initial discharge capacity of only 129 mAh g^{-3} at 0.1 C and unsatisfactory rate capability, resulting from the low electronic conductivity [11]. Shi et al. [7] reported that substitution of a small quantity of Li$^+$ in LiFePO$_4$ by Cr^{3+} could greatly enhance the material's electronic conductivity, thus the material's reversible capacity and rate capability could be obviously improved. In this work, we synthesized spherical Li$_{0.97}$Cr$_{0.01}$FePO$_4$/C composite cathode material with the inexpensive Fe(NO$_3$)$_3$ as iron source and sucrose as reductive agent and carbon source via controlled crystallization—carbothermal reduction method. Compared with the previous spherical carbon-coated LiFePO$_4$ [11], the tap-density, reversible capacity and rate capability of the spherical Li$_{0.97}$Cr$_{0.01}$FePO$_4$/C were obviously improved.

2. Experimental

First, spherical amorphous FePO$_4 \cdot x$H$_2$O powders were synthesized by controlled crystallization method, using Fe(NO$_3$)$_3$, H$_3$PO$_4$ and NH$_3$ as the raw materials, according to the reaction:

$$Fe(NO_3)_3 + H_3PO_4 + 3NH_3 + xH_2O$$

$$= FePO_4 \cdot xH_2O + 3NH_4NO_3 \tag{1}$$
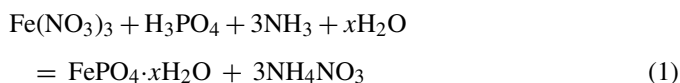
The reactor is illustrated in Fig. 1. The spherical FePO$_4 \cdot x$H$_2$O was synthesized as the follows. The mixed solution of Fe(NO$_3$)$_3$ and H$_3$PO$_4$ was pumped continuously into the reactor. At the same time, the solution of NH$_3$ was also pumped into the reactor to control the pH of the mixture. The concentration of the two solutions, average rest time (or the feed-in velocity), agitating intensity, temperature, and pH of the mixture being agitating vigorously in the reactor should be controlled carefully. Thus, the growth of FePO$_4 \cdot x$H$_2$O particles in the reactor could be controlled effectively. The irregular particles changed gradually into spherical particles after enough time of reaction and agitation. The mixture in the reactor was filtered, washed and dried. Thus, the spherical FePO$_4 \cdot x$H$_2$O powders were obtained.
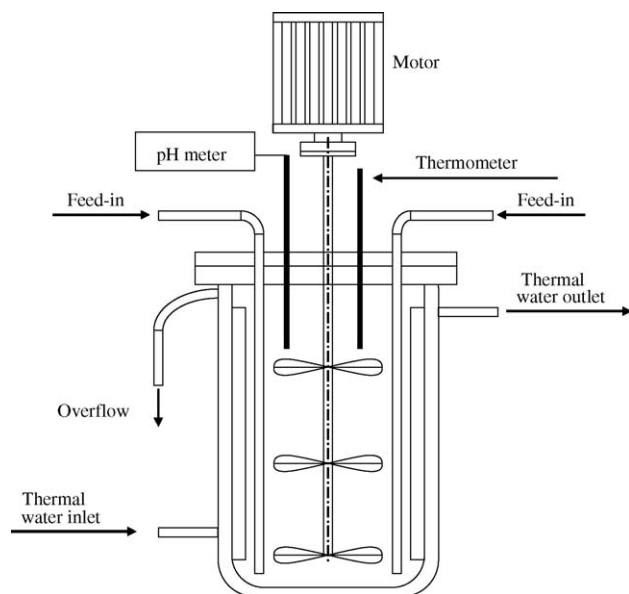

Fig. 1. Schematic diagram of the reactor for controlled crystallization process.

In this work, the controlled crystallization parameters were as follows. The concentration of the Fe(NO$_3$)$_3$ and H$_3$PO$_4$ solution were both 1.0 mol L^{-1}. The concentration of the NH$_3$ solution was 3.0 mol L^{-1}. The agitating intensity was 50–60 W L^{-1}. The average rest time was 8–12 h. The temperature was 45 °C. The pH was 2.1.

The spherical amorphous FePO$_4 \cdot x$H$_2$O powders were preheat treated at 520 °C for 20 h in air to obtain spherical anhydrous FePO$_4$ powders.

To synthesize spherical carbon-coated Li$_{0.97}$Cr$_{0.01}$FePO$_4$ powders, we will mix spherical FePO$_4$ precursors, Li$_2$CO$_3$, Cr(NO$_3$)$_3$ and sucrose (C$_{12}$H$_{22}$O$_{11}$) uniformly. However, if we use the traditional mechanically mixing methods, such as ball milling, the uniform spherical FePO$_4$ particles will be broken to pieces. Thus, to keep FePO$_4$ precursor and Li$_{0.97}$Cr$_{0.01}$FePO$_4$/C product particles as ideal spheres, we have to use special mixing methods. In this work, Li$_2$CO$_3$, Cr(NO$_3$)$_3$, sucrose (C$_{12}$H$_{22}$O$_{11}$) and deionized water (H$_2$O) were firstly mixed in a molar ratio of Li$_2$CO$_3$:Cr(NO$_3$)$_3$:C$_{12}$H$_{22}$O$_{11}$:H$_2$O = 0.485:0.01:0.1:2 and ball milled for 4 h in a planetary miller. A kind of uniform slurry was obtained. Then, we added spherical FePO$_4$ powders in a molar ratio of FePO$_4$:Li$_2$CO$_3$ = 1:0.485 into the slurry and agitated the mixture vigorously. In the eventually obtained homogeneous slurry, the FePO$_4$ particles kept the original spheres, while the fine particles of Li$_2$CO$_3$, Cr(NO$_3$)$_3$, and C$_{12}$H$_{22}$O$_{11}$ were uniformly coated on the surface of spherical FePO$_4$ particles or filled up the vacancies among the spherical FePO$_4$ particles. The mixed slurry was dried and then sintered at 800 °C for 16 h in N$_2$. The spherical carbon-coated Li$_{0.97}$Cr$_{0.01}$FePO$_4$ powders were finally obtained through carbothermal reduction process. During the sintering process, the reactions may be very complex. We assume the carbothermal reaction can be approximately written as the formula below (omit the small quantity of Cr(NO$_3$)$_3$). According to the formula, the obtained composite will be Li$_{0.97}$Cr$_{0.01}$FePO$_4$/0.7 C. The calculated residual carbon

content is about 5 wt.%.

$$0.5Li_2CO_3 + FePO_4 + 0.1C_{12}H_{22}O_{11}$$
$$= LiFePO_4 + 0.5CO_2 + 0.5CO + 0.7C + 1.1H_2O \qquad (2)$$
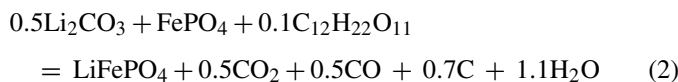
The Fe/P molar ratio of the precursors synthesized by controlled crystallization method was analyzed by ICP. DTA/TGA of $FePO_4 \cdot xH_2O$ was used to direct the pre-heat treatment. Powder X-ray diffraction (XRD, D/max-rB) using Cu Kα radiation was used to identify the crystalline phase and crystal lattice parameters of the $FePO_4 \cdot xH_2O$, $FePO_4$ and $Li_{0.97}Cr_{0.01}FePO_4/C$ powders. The sample morphology was observed by field emission scanning electron microscopy (SEM, JSM6301F). The surface elements' content of spherical $Li_{0.97}Cr_{0.01}FePO_4/C$ powders were determined by X-ray photoelectron spectroscopy (XPS, PHI-5300 ESCA). The powders' particle size distribution was identified by laser particle size analyzer (OMEC LS-POP(III)). The tap-density and carbon content of the powders were tested using the method described in Ref. [11].

Experimental test cells for measurements used the cathode with the composition of 80 wt.% $Li_{0.97}Cr_{0.01}FePO_4/C$, 10 wt.% carbon black, and 10 wt.% PTFE. The separator was a Celguard 2400 microporous polypropylene membrane. The electrolyte was 1M $LiPF_6$ EC + DEC (1:1 by volume). A lithium metal anode was used in this study. The cells were assembled in a glove box filled with argon gas. The charge–discharge cycling was galvanostatically performed at a current of 0.005, 0.05, 0.1, 0.25 and 1.0 C with cut-off voltages of 2.5–4.2 V (versus Li/Li$^+$) at 20 °C.

3. Results and discussion

3.1. The Fe/P molar ratio of the precursors in relation to pH during controlled crystallization process

In order to obtain spherical $Li_{0.97}Cr_{0.01}FePO_4/C$ powders, the stoichiometric $FePO_4$ powders are considered as the necessary precursor according to our previous experiments. It is very important to insure the Fe/P molar ratio of the precursors synthesized by controlled crystallization method is 1.

It is well known that Fe^{3+} is easy to hydrolyze to $Fe(OH)^{2+}$, $Fe(OH)_2^+$ and $Fe(OH)_3$ when the solution's pH increases, while PO_4^{3-} is easy to hydrolyze to HPO_4^{2-}, $H_2PO_4^-$ when the solution's pH decreases. Thus, different pH of the mixture in the reactor will lead to different products during controlled crystallization process, using $Fe(NO_3)_3$, H_3PO_4 and NH_3 as the raw materials. Fig. 2 shows the Fe/P molar ratio of the precursors in relation to pH. When pH is less than 1.95, the Fe/P molar ratio is less than 1. When pH is larger than 2.25, the Fe/P molar ratio is larger than 1. When pH is between 1.95 and 2.25, the Fe/P molar ratio is very close to 1. Based on the results, in this work, we fixed the pH on 2.1. The formula of the precursor obtained at pH 2.1 can be written as $FePO_4 \cdot xH_2O$.
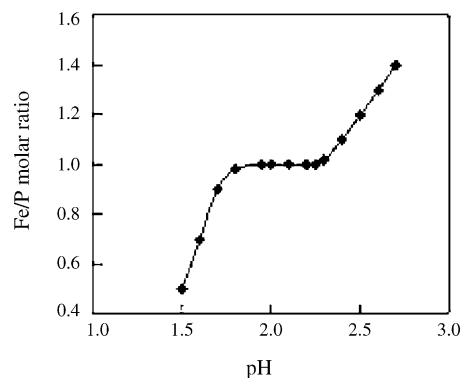

Fig. 2. The Fe/P molar ratio of the precursors prepared at different pH.

3.2. Pre-heat treatment of the $FePO_4 \cdot xH_2O$ precursor

The spherical $FePO_4 \cdot xH_2O$ precursor obtained at pH 2.1 is amorphous. The water content of $FePO_4 \cdot xH_2O$ is not fixed. According to our analysis, the value of x is about 2.5, but varies slightly with drying condition, particle size distribution, etc. To insure the accuracy of the proportion of raw materials batch to batch, the anhydrous stoichiometric $FePO_4$ is preferred to. The anhydrous stoichiometric $FePO_4$ can be obtained from pre-heat treatment of $FePO_4 \cdot xH_2O$.

Fig. 3 shows the TGA–DTA curves of the $FePO_4 \cdot xH_2O$ powders with a heating rate of 10 °C min^{-1} from room temperature to 580 °C in air. On the DTA curve near 178 °C, there is a very strong endothermic peak, associating with the sharply weight loss on the TGA curve, which is related to the quickly dehydration of $FePO_4 \cdot xH_2O$. During 178–500 °C, the TGA curve indicates the slowly elimination of residual H_2O in $FePO_4 \cdot xH_2O$. When the temperature is high than 500 °C the TGA curve indicates the weight remains constant. We can conclude that the dehydration of $FePO_4 \cdot xH_2O$ will finish and the powders' composition will be confirmed when the pre-heat treating temperature is high than 500 °C. On the DTA curve near 475 °C, there is a strong exothermic peak, which is related to the transformation of the amorphous $FePO_4$ to hexagonal $FePO_4$ crystal.

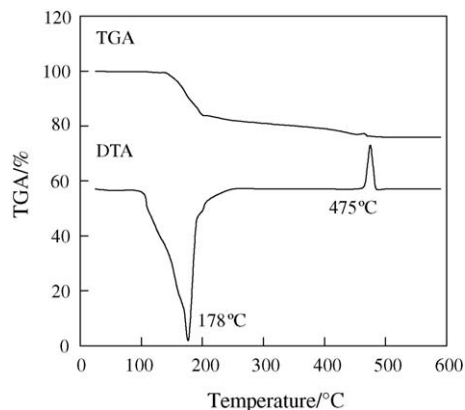Based on the above analysis, we pre-heat treated the $FePO_4 \cdot xH_2O$ powders at 520 °C for 20 h in air to

Fig. 3. DTA/TGA curves of the $FePO_4 \cdot xH_2O$.

obtain anhydrous hexagonal $FePO_4$ powders, which were used as the precursors to synthesize $Li_{0.97}Cr_{0.01}FePO_4/C$ powders.

3.3. XRD analysis of $FePO_4 \cdot xH_2O$, $FePO_4$ and $Li_{0.97}Cr_{0.01}FePO_4/C$ powders

Fig. 4 shows the XRD patterns of the $FePO_4 \cdot xH_2O$, $FePO_4$ and $Li_{0.97}Cr_{0.01}FePO_4/C$ powders. There are no identifiable peaks on the XRD spectra of $FePO_4 \cdot xH_2O$ powders, indicating $FePO_4 \cdot xH_2O$ synthesized by controlled crystallization process is amorphous. There are strong and sharp peaks on the $FePO_4$ powders' XRD spectra, which is almost the same as the XRD spectra of anhydrous hexagonal structured $FePO_4$ (JCPDS card no. 29-0715). The crystal lattice parameters calculated by the XRD data are $a = 5.034$ Å, $b = 5.034$ Å, $c = 11.246$ Å. The spectra proves the amorphous $FePO_4 \cdot xH_2O$ powders pre-heat treated at 520 °C for 20 h were well crystallized into phase-pure anhydrous hexagonal $FePO_4$ powders. The spectra of $Li_{0.97}Cr_{0.01}FePO_4/C$ is almost the same as the spectra of pure ordered orthorhombic olivine structured $LiFePO_4$ (JCPDS card no. 40-1499). The absence of any other signals indicates there are no unwanted impurity phases, such as Li_3PO_4 and Fe^{3+} related compounds. There is no evidence of diffraction peaks for carbon, indicating the residual pyrolytic carbon in product is amorphous. The crystal lattice parameters calculated by the XRD data of the material are $a = 6.008$ Å, $b = 10.328$ Å and $c = 4.693$ Å.

According to X-ray diffraction analysis, $FePO_4$ and $Li_{0.97}Cr_{0.01}FePO_4/C$ have similar structure. During sintering the mixture of $FePO_4$, Li_2CO_3, $Cr(NO_3)_3$ and sucrose in N_2, the $FePO_4$ framework approximately holds the line, while the Li^+ and Cr^{3+} diffuse into $FePO_4$ spheres and insert into the $FePO_4$ framework. At the same time, the sucrose will pyrolyse. The hydrogen and carbon generated from sucrose can produce a strong reductive atmosphere for the reduction of Fe^{3+} to Fe^{2+}, resulting the synthesis of $Li_{0.97}Cr_{0.01}FePO_4$. The residual pyrolytic carbon will coat on the spherical $Li_{0.97}Cr_{0.01}FePO_4$ particles to form the composite $Li_{0.97}Cr_{0.01}FePO_4/C$.
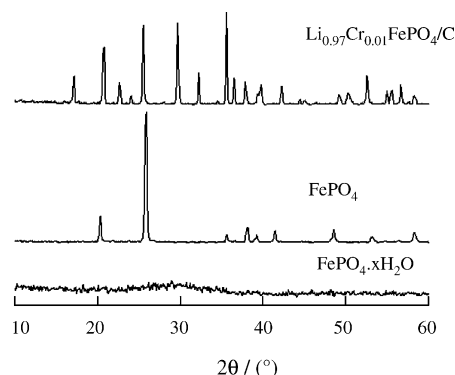
3.4. Morphology of $FePO_4 \cdot xH_2O$, $FePO_4$ and $Li_{0.97}Cr_{0.01}FePO_4/C$ powders

The morphology of $FePO_4 \cdot xH_2O$ and $FePO_4$ powders is very similar. The powders are both composed of well-dispersed spherical particles, as shown in Fig. 5(a) and (c). Each of the spherical particles is made up of a large number of small grains, as shown in Fig. 5(b) and (d). Fig. 5(e) shows the $Li_{0.97}Cr_{0.01}FePO_4/C$ powders are mainly composed of spherical particles similar to the $FePO_4$ precursors, although there are slight agglomeration and a small quantity of fragments. Fig. 5(f) shows the spherical $Li_{0.97}Cr_{0.01}FePO_4/C$ particle is wholly coated by some substance whose composition is mainly carbon, proved by EDS and XPS analysis. The crystalline grains cannot be observed because of the coated carbon layer. There are also some carbon fragments adhering to the spherical particle.

3.5. XPS analysis of the $Li_{0.97}Cr_{0.01}FePO_4/C$ powders

The carbon content of the $Li_{0.97}Cr_{0.01}FePO_4/C$ powders is about 6 wt.%, determined by the method described in Ref. [11]. In other words, the molar ratio of $C:Li_{0.97}Cr_{0.01}FePO_4$ is about 0.8. The tested carbon content (6 wt.%) is close to the calculated data (5 wt.%), indicating the assumed carbothermal reduction formula mentioned in the experimental part is correct in the rough. However, according to XPS analysis, on the surface of $Li_{0.97}Cr_{0.01}FePO_4/C$ powders, the molar ratio of C:Li:Fe:P is about 40:1:1:1. The result indicates the surface composition is mainly the carbon. The pyrolytic carbon is coated the surface of spherical $Li_{0.97}Cr_{0.01}FePO_4$ particles rather perfectly, which accords with the SEM analysis.

3.6. Particle size distribution and tap-density of the spherical $FePO_4 \cdot xH_2O$, $FePO_4$ and $Li_{0.97}Cr_{0.01}FePO_4/C$ powders

As shown in Table 1, the tap-density of the spherical $Li_{0.97}Cr_{0.01}FePO_4/C$ powders prepared in this work is as high as 1.8 g cm^{-3}, which is remarkably higher than the non-spherical $LiFePO_4$ powders reported, whose tap-density is usual 1.0–1.4 g cm^{-3}. Compared with the previous spherical carbon-coated $LiFePO_4$ powders (the tap-density is 1.6 g cm^{-3}) [11], the spherical $Li_{0.97}Cr_{0.01}FePO_4/C$ powders prepared in this work have higher tap-density, mainly because of the better spherical quality. The high-density spherical $Li_{0.97}Cr_{0.01}FePO_4/C$ cathode material can be used in the lithium ion batteries to greatly increase the batteries' energy density. According to our expe-

Fig. 4. XRD patterns of the $FePO_4 \cdot xH_2O$, $FePO_4$, $Li_{0.97}Cr_{0.01}FePO_4/C$ powders.

Table 1
The particle size distribution and tap-density of the spherical $FePO_4 \cdot xH_2O$, $FePO_4$ and $Li_{0.97}Cr_{0.01}FePO_4/C$

Spherical powders	D_{10} (μm)	D_{50} (μm)	D_{90} (μm)	Tap density (g cm^{-3})
$FePO_4 \cdot xH_2O$	4.4	10.8	19.1	1.1
$FePO_4$	4.2	9.9	15.8	1.5
$Li_{0.97}Cr_{0.01}FePO_4/C$	3.2	8.0	14.4	1.8
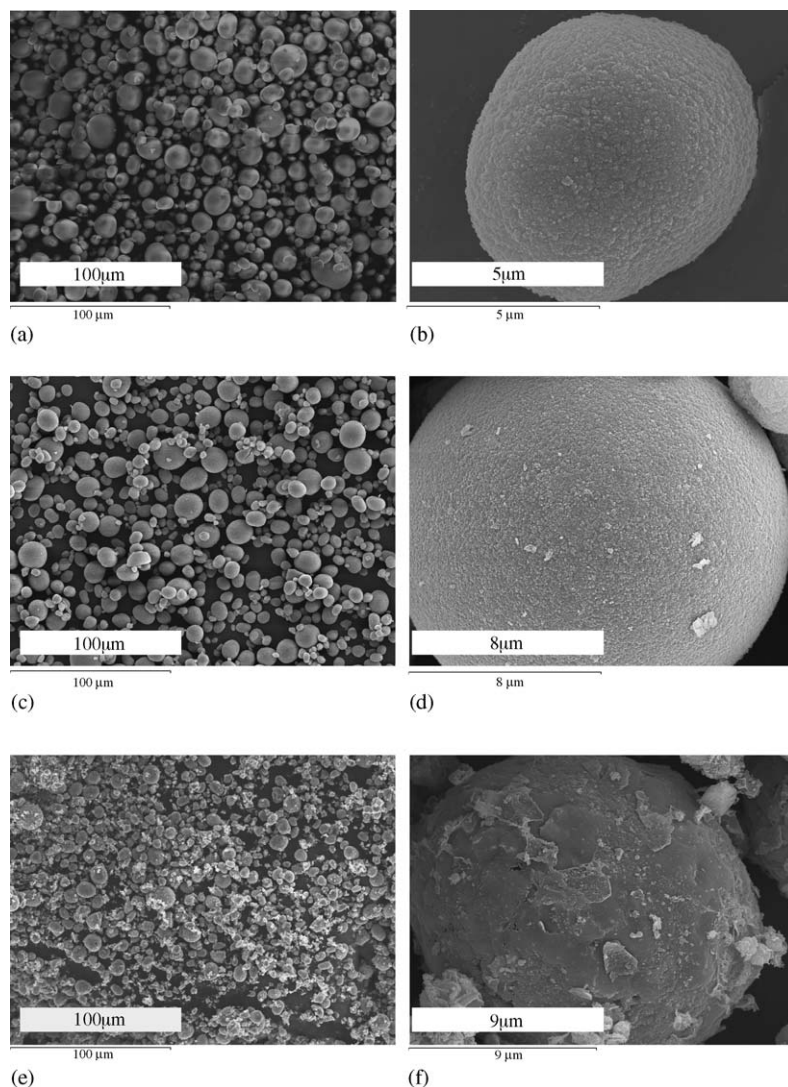
Fig. 5. SEM images of the spherical $FePO_4 \cdot xH_2O$, $FePO_4$ and $Li_{0.97}Cr_{0.01}FePO_4/C$: (a) $FePO_4 \cdot xH_2O$ powders, (b) a spherical $FePO_4 \cdot xH_2O$ particle, (c) $FePO_4$ powders, (d) a spherical $FePO_4$ particle, (e) $Li_{0.97}Cr_{0.01}FePO_4/C$ powders and (f) a spherical $Li_{0.97}Cr_{0.01}FePO_4/C$ particle.

rience, the powders' tap-density can be further improved by two possible ways. One is to optimize the precursors' spherical quality and particle size distribution through adjusting the controlled crystallization parameters. The other is to improve the pyrolytic carbon's coating quality, especially to eliminate the carbon fragments adhering to the spherical particles. The carbon sources, mixing procedure, and the carbothermal reduction process should be optimized. We will report the results elsewhere.

3.7. Electrochemical performance of the spherical $Li_{0.97}Cr_{0.01}FePO_4/C$ cathode material

Fig. 6 presents the initial and 100th charge discharge curves of the $Li_{0.97}Cr_{0.01}FePO_4/C$ composite at current of 0.1 C. A flat charge discharge curve around 3.45 V over a large compositional range implies that the two-phase redox reaction proceeds via a first-order transition between $LiFePO_4$ and $FePO_4$ [1]. The small voltage difference between the charge and discharge plateaus is representative of its good kinetics. The composite cathode mate-

rial has a first cycle charge capacity of 152 mAh g^{-1} followed by a discharge capacity of 142 mAh g^{-1}, and the rather high initial charge discharge efficiency of 93.4%. After 100 cycles, the reversible discharge capacity is 138 mAh g^{-1}, showing the
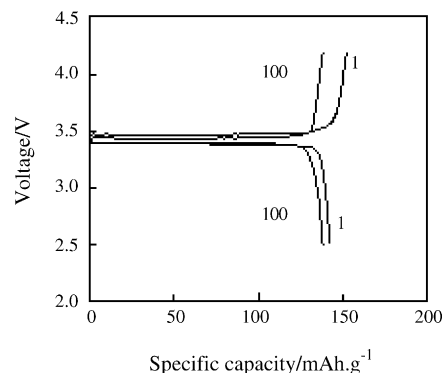

Fig. 6. Charge–discharge curves of the initial and 100th cycle of $Li_{0.97}Cr_{0.01}FePO_4/C$ at 0.1 C.

Table 2
Electrochemical performance of the spherical $Li_{0.97}Cr_{0.01}FePO_4/C$

Charge–discharge current (C)	0.005	0.05	0.1	0.25	1.0
Initial charge specific capacity (mAh g^{-1})	165	157	152	146	130
Initial discharge specific capacity (mAh g^{-1})	163	151	142	131	110
Initial charge–discharge efficiency (%)	98.8	96.2	93.4	89.7	84.6
Discharge specific capacity at 100th cycle (mAh g^{-1})	162[a]	149[a]	138	127	105
Capacity retention after 100 cycles (%)	99.4[a]	98.7[a]	97.2	96.9	95.5

[a] Fifth cycle at 0.005 C and 50th cycle at 0.05 C.
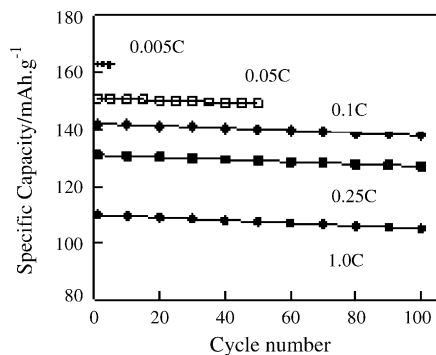

Fig. 7. Cycling performance of the $Li_{0.97}Cr_{0.01}FePO_4/C$ at different current.

retention of 97.2%. At current of 0.005, 0.05, 0.25 and 1.0 C, the charge–discharge curves are similar to Fig. 6. The related data of electrochemical performance is illustrated in Table 2. Both Table 2 and Fig. 7 show excellent cycling performance of the $Li_{0.97}Cr_{0.01}FePO_4/C$ composite at different current. The good cycling behavior is attributed to the enhancement of the electronic conductivity by the Cr^{3+} substitution, carbon coating, and also to the excellent cycle ability of $LiFePO_4$ itself duo to the high stability of the olivine structure and the minor lattice adjustments upon cycling [12].

Fig. 8 shows the initial discharge curves of the $Li_{0.97}Cr_{0.01}FePO_4/C$ at different current. At 0.005 C, the discharge capacity of 163 mAh g^{-1} is very close to the theoretical capacity of $LiFePO_4$ (170 mAh g^{-1}), which indicates that the active material utilization is very close to the theoretical value. However, the capacity decreases obviously while the current increases. At 1.0 C, the discharge capacity is only 110 mAh g^{-1}. The result indicates the rate capability of the prepared $Li_{0.97}Cr_{0.01}FePO_4/C$ composite cathode material should

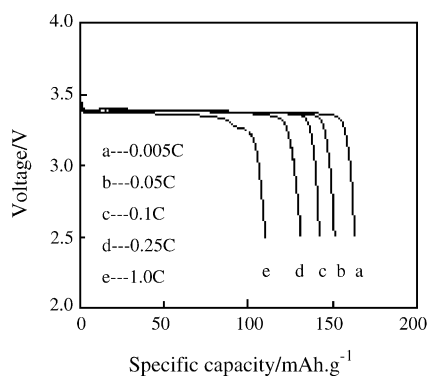be further improved, although Cr^{3+} substitution and carbon coating have improved the material's performance at a certain extent, comparing to the previous spherical $LiFePO_4$ [11].

During sintering the mixture of $FePO_4$, Li_2CO_3, $Cr(NO_3)_3$ and sucrose in N_2, the sucrose and pyrolytic carbon are difficult to diffuse into the close-grained $FePO_4$ spheres. The conductive pyrolytic carbon is only coated on the surface. On the other hand, though the Li^+ and Cr^{3+} can both diffuse into $FePO_4$ spheres and insert into the $FePO_4$ framework, the diffusion and insertion of Cr^{3+} is more difficult because of its high positive charge density. We believe in the core of $Li_{0.97}Cr_{0.01}FePO_4/C$ sphere, there is no or at least lack of Cr^{3+} substitution. Based on the above analysis, we can conclude the $Li_{0.97}Cr_{0.01}FePO_4/C$ spheres may have the high electronic conductive surface and poor electronic conductive core. This is the reason for the unsatisfactory rate capability of the spherical $Li_{0.97}Cr_{0.01}FePO_4/C$ composite material.

One effective way is expected to solve the above problem. We can dope Cr^{3+} and suitable carbon sources homogeneously in the whole amorphous $FePO_4 \cdot xH_2O$ spheres by coprecipitation during the controlled crystallization process. Using the Cr^{3+} and carbon sources doped $FePO_4 \cdot xH_2O$ precursors, we can obtain the spherical $Li_{0.97}Cr_{0.01}FePO_4/C$ powders with high electronic conductivity and high rate capability because of the homogeneous distribution of Cr^{3+} substitution and conductive pyrolytic carbon in the whole spheres (from surface to core). The research work is now carrying on in our laboratory. We will report the results elsewhere.

4. Conclusions

The spherical $Li_{0.97}Cr_{0.01}FePO_4/C$ composite cathode material has been synthesized via a controlled crystallization—carbothermal reduction method. At current of 0.005, 0.05, 0.1, 0.25 and 1.0 C, the cathode materials have initial discharge specific capacity of 163, 151, 142, 131 and 110 mAh g^{-1}, respectively. The materials also show excellent cycling performance. The tap-density of the spherical $Li_{0.97}Cr_{0.01}FePO_4/C$ powders is as high as 1.8 g cm^{-3}, which is remarkably higher than the non-spherical $LiFePO_4$ powders reported. The high-density spherical $Li_{0.97}Cr_{0.01}FePO_4/C$ cathode material provides significant incentive for battery manufacturers to consider it as a very promising candidate to be used in the lithium ion batteries with high power density.

The controlled crystallization—carbothermal reduction method proposed in this work has a lot of advantages, such as low cost of raw materials, simple synthesis process, easiness of mass production, etc. We expect the new process can also

Fig. 8. Initial discharge curves of the $Li_{0.97}Cr_{0.01}FePO_4/C$ at different current.

be used to further improve the material's pile density and rate capability. Further studies in this field are very promising and significative.

Acknowledgements

References

[1] A.K. Padhi, K.S. Nanjundaswamy, J.B. Goodenough, J. Electrochem. Soc. 144 (1997) 1188.
[2] K.S. Park, J.T. Son, H.T. Chung, et al., Solid State Commun. 129 (2004) 311.
[3] Y.K. Chen, S. Okada, J. Yamaki, Compos. Interf. 11 (2004) 277.
[4] C.H. Mi, G.S. Cao, X.B. Zhao, Mater. Lett. 59 (2005) 127.
[5] K. Konstantinov, S. Bewlay, G.X. Wang, et al., Electrochim. Acta 50 (2004) 421.
[6] S.Y. Chung, J.T. Bloking, Y.M. Chiang, Nat. Mater. 1 (2002) 123.
[7] S.Q. Shi, L.J. Liu, C.Y. Ouyang, et al., Phys. Rev. B 68 (2003) 195108.
[8] K.S. Park, K.T. Kang, S.B. Lee, et al., Mater. Res. Bull. 39 (2004) 1803.
[9] J.R. Ying, C.R. Wan, C.Y. Jiang, et al., J. Power Sources 99 (2001) 78.
[10] J.R. Ying, C.Y. Jiang, C.R. Wan, J. Power Sources 129 (2004) 264.
[11] M. Lei, Preparation and Characterization of LiFePO$_4$ Cathode Material for Lithium-Ion Batteries, Dissertation, Institute of Nuclear and New Energy Technology, Tsinghua University, Beijing, 2005.
[12] A. Yamada, S.C. Chung, K. Hinokuma, J. Electrochem. Soc. 148 (2001) A224.